

Selectivity-Controlling Factors in Catalytic Methanol Amination Studied by Isotopically Modulated Excitation IR Spectroscopy

Nobutaka Maeda,^{†,*} Fabian Meemken,[†] Konrad Hungerbühler,[†] and Alfons Baiker^{†,‡,*}

[†]Institute for Chemical and Bioengineering, Department of Chemistry and Applied Biosciences, ETH Zurich, Hönggerberg, HCI, CH-8093 Zurich, Switzerland

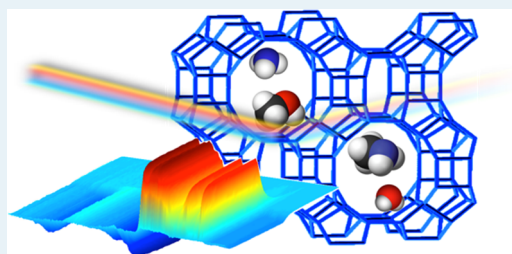
[‡]Chemistry Department, Faculty of Science, King Abdulaziz University, P.O. Box 80203, Jeddah 21589, Saudi Arabia

Supporting Information

ABSTRACT: Present mechanistic models for catalytic amination of methanol by zeolites focus on shape-selectivity of monomethylamine (MMA), dimethylamine (DMA), and trimethylamine (TMA) in the micropores. However, a rational explanation of the uniquely high selectivity to MMA and DMA achieved over Na⁺-exchanged mordenite (Na⁺-MOR) requires the consideration of additional selectivity-controlling factors. We have applied modulation–excitation diffuse reflectance IR Fourier transform spectroscopy with periodic perturbation by the isotope CD₃OD to realize a chemically steady state but isotopically transient condition during methylamines synthesis from methanol and ammonia.

These studies proved that the H-bonded network of methanol agglomerates and open dimers in the micropores can readily be replaced by NH₃ at 623 K, probably leading to a decrease in the methanol concentration around catalytically active sites and, thus, suppressing the consecutive reaction of MMA to DMA and, finally, to TMA. Concentration modulation between NH₃ and MMA indicated weaker adsorption of MMA, which was largely replaced by NH₃ at the reaction temperature, thereby hindering further methylation of MMA.

KEYWORDS: ammonia, *in situ* IR spectroscopy, isotope, methanol, methylamines, mordenite



Lower aliphatic amines, methylamine (MMA), and dimethylamine (DMA) are widely used chemical intermediates for producing pesticides, pharmaceuticals, surfactants, and solvents. Over 1 million tons of methylamines are annually produced by catalytic reaction of methanol with ammonia.¹ Various solid acid catalysts have been reported to be suitable for the synthesis of methylamines,^{2–6} among which amorphous silica–alumina mixed oxides are most widely used in industry. Thermodynamically, trimethylamine (TMA) is the preferred product because MMA and DMA easily disproportionate to NH₃ and TMA at reaction conditions. High commercial demand on MMA and DMA has spurred both industrial and academic research on designing selective catalytic materials. Zeolites with suitable micropores were reported to offer shape-selectivity of MMA (0.37 × 0.39 × 0.44 nm), DMA (0.39 × 0.47 × 0.60 nm), and TMA (0.39 × 0.54 × 0.61 nm).⁷ In particular, Na⁺-exchanged mordenite (Na⁺-MOR) with a pore size of 0.26 × 0.57 nm (8-membered ring) and 0.65 × 0.70 nm (12-membered ring) shows excellent selectivity to MMA (42.1%).⁸ Interestingly, proton-exchanged mordenite (H⁺-MOR) with the same pore size exhibits poor selectivity to MMA (7.2%).⁹ Therefore, the shape selectivity or acid strength alone cannot explain the unique selectivity of Na⁺-MOR catalysts, and other selectivity-controlling factors need to be considered for fine-tuning active centers and their surroundings.

In situ diffuse reflectance IR Fourier transform spectroscopy (DRIFTS) is a powerful technique to investigate catalytic solid–gas interfaces under actual working, i.e., operando conditions.¹⁰ Especially, its combination with a transient spectroscopic technique is often highly advantageous compared with steady-state spectroscopic techniques.¹¹ Recently, the combination of *in situ* DRIFTS with steady state isotopic transient kinetic analysis (SSITKA)^{11–14} or modulation excitation spectroscopy (MES)^{15,16} was shown to offer great potential for investigating kinetics of surface processes. Here, we combined SSITKA with MES to enhance the signal-to-noise (S/N) ratio of IR signal changes during isotope modulation and extracted kinetic information by phase-sensitive detection (PSD).^{15,16} Concentration modulation and isotope modulation as an external stimulation were applied to create chemically or isotopically transient catalytic solid–gas interfaces, providing molecular insight into the synthesis of methylamines occurring in the MOR micropores.

Figure 1a and c shows phase- and time-domain IR spectra during isotope modulation (CD₃OD ↔ CH₃OH) over Na⁺-exchanged MOR (Na⁺-MOR) at 623 K. The phase-domain spectra were obtained by converting the time-resolved spectra (see the Experimental Section). Bands at 2951 and 2850 cm⁻¹

Received: August 16, 2012

Revised: January 10, 2013

Published: January 11, 2013

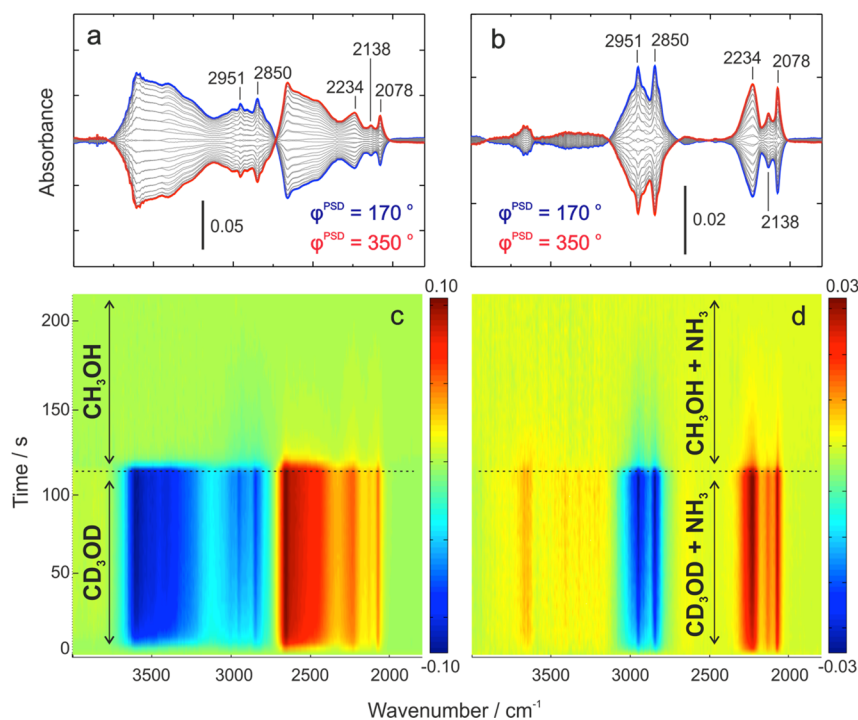


Figure 1. (a, b) Phase- and (c, d) time-domain IR spectra during isotope modulation at 623 K; (a, c) $\text{CD}_3\text{OD} \leftrightarrow \text{CH}_3\text{OH}$, (b, d) $\text{CD}_3\text{OD} + \text{NH}_3 \leftrightarrow \text{CH}_3\text{OH} + \text{NH}_3$.

are assigned to the ν_9 , $\nu(\text{CH}_3)_{\text{as}} \text{A}''$, and ν_3 , $\nu(\text{CH}_3)_s \text{A}'$, fundamental vibrations of CH_3OH and methoxide species (CH_3O^-).^{17,18} Weak shoulders around 2951 cm^{-1} originate from ν_2 , $\nu(\text{CH}_3)_{\text{as}} \text{A}'$ (2996 cm^{-1}), and $\nu_4 + \nu_{10}$, $\nu(\text{CH}_3) + \delta(\text{CH}_3) \text{A}''$ (2911 cm^{-1}).¹⁷ Note that the direction of dipole moment derivatives is perpendicular to the C–O–H plane for the A'' vibrations and in the plane for the A' vibrations. Similarly CD_3OD showed the ν_3 vibration at 2078 cm^{-1} , and ν_9 , ν_2 , and $\nu_4 + \nu_{10}$ vibrations overlapped each other, centered at 2234 cm^{-1} . Because of the isotope effect, overtone, $2\nu_5$ ($2\delta(\text{CD}_3) \text{A}'$), was clearly observable at 2138 cm^{-1} .¹⁷ In the region of 3200–3700 and 2350–2700 cm^{-1} , broad bands assignable to the ν_1 vibrations, that is, $\nu(\text{OH})$ and $\nu(\text{OD})$, emerged. Major O–H and O–D components are centered sharply at 3598 and 2655 cm^{-1} , which implies the H-bonded vibration in the methanol open dimer.^{19–21} In the Na^+ -MOR pores, the band position shifted to a higher wavenumber (blue shift), compared with the gas-phase open dimer (3558 cm^{-1}), possibly because of the weak interaction with oxide walls of the pores. The open dimer can be formed only at temperatures higher than 673 K in the gas-phase.¹⁹ Probably, the geometric and electronic structure of the zeolite channels allows its formation at the reaction condition (623 K).

In contrast, the presence of NH_3 during isotope modulation showed a striking difference in the IR spectra (Figure 1b and d). The bands arising from the CH_3 and CD_3 vibrations of methanol dimers and agglomerates almost disappeared in the presence of NH_3 (compare Figure 1, a and b). Apparently, the H-bond network of the methanol agglomerates typically existing in gas or liquid phase is broken in the Na^+ -MOR pores and replaced by NH_3 molecules. This suggests that the Na^+ -MOR pores are predominantly occupied by NH_3 molecules, together with small amounts of MMA and MeOH. At higher conversions, DMA and TMA species may also be present. Methoxide species originating from methanol

adsorption are considered to be bound to the Na^+ atom.²² A feasible scenario is that exchange of H or R groups of adsorbed NH_3 (MMA, DMA) occurs by reaction with MeOH or possibly also by disproportionation of adsorbed amines. The dominance of adsorbed NH_3 resulting in a reduced concentration of methanol and methoxide species seems to suppress further methylation of MMA to DMA and TMA, leading together with the shape-selectivity induced by the geometric dimensions of MOR pores to high selectivity to MMA. This scenario is also supported by the fact that a high $\text{NH}_3/\text{CH}_3\text{OH}$ ratio in the gas phase offers better selectivity to MMA for many catalysts.^{3,4,23}

The same isotope modulation experiment in the presence of NH_3 at 523 K (Figure 2a and b) provides unique insight into catalytic activity and selectivity of the Na^+ -MOR catalyst. In contrast to the experiment performed at 623 K (Figure 1b), the methanol open dimer and some methanol aggregates could be detected in the Na^+ -MOR pores. It appears that the H-bond network is difficult to break inside the Na^+ -MOR pores, and hence, NH_3 molecules have less access to the catalytically active sites. Na^+ -MOR is reported to exhibit high activity at temperatures higher than 523 K and also to offer better selectivity to MMA at higher temperatures.⁸ This activity and selectivity enhancement can be well explained by the cleavage of the H-bond network of methanol, which in turn is replaced by NH_3 .

In addition to the isotope modulation, a concentration modulation experiment, that is, periodically changing the concentration of NH_3 (16.7 vol % \leftrightarrow 0 vol %) in the presence of CH_3OH (16.7 vol %), gave further clues to the exceptionally high selectivity to MMA of Na^+ -MOR. Figure 3 shows the concentration profiles (mass spectroscopy signal) in the gas phase during $\text{NH}_3 + \text{CH}_3\text{OH} \leftrightarrow \text{CH}_3\text{OH}$ cycles at 623 K. Upon admission of NH_3 , methylamines were formed periodically without any deterioration of the catalytic activity during six cycles. Because the concentration of methanol was kept

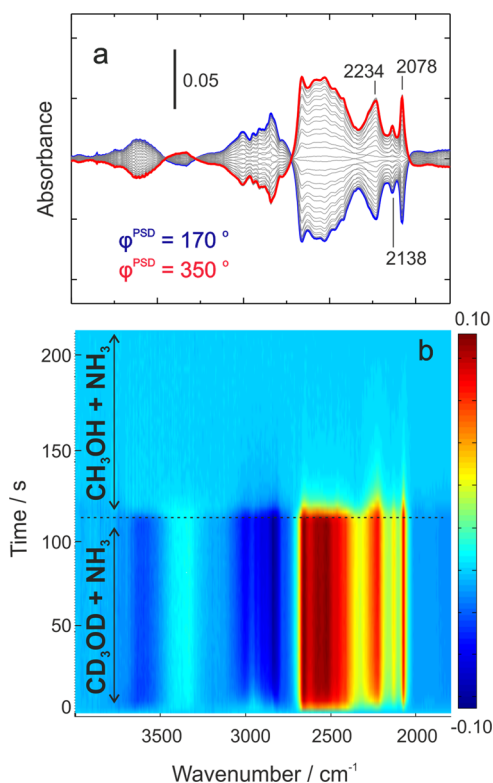


Figure 2. (a) Phase- and (b) time-domain IR spectra during isotope modulation ($\text{CD}_3\text{OD} + \text{NH}_3 \leftrightarrow \text{CH}_3\text{OH} + \text{NH}_3$) at 523 K.

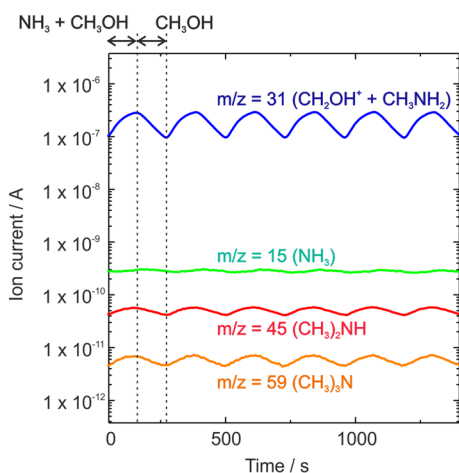


Figure 3. MS signals of the gas-phase components during NH_3 modulation ($\text{NH}_3 + \text{CH}_3\text{OH} \leftrightarrow \text{CH}_3\text{OH} + \text{NH}_3$) at 623 K.

constant, the oscillation of m/z (mass-to-charge ratio) = 31 originated mainly from the concentration change of MMA. The steady signal of $m/z = 15$ implies that almost all the NH_3 was consumed. Previous methanol amination studies⁸ on Na^+ -MOR showed that hardly any dimethyl ether is formed when methanol and ammonia are passed over Na^+ -MOR, which is in agreement with our observation. However, it has to be stressed that our spectroscopic cell behaves like a differential reactor at low conversion, and therefore, possible formation of some dimethyl ether at high conversion cannot be ruled out.

During the NH_3 modulation experiment, in situ IR spectra were also recorded; the phase-domain spectra are shown in Figure 4. The spectra demonstrate the exchange of molecules ($\text{NH}_3 \leftrightarrow \text{CH}_3\text{OH}$) in the pores; the bands of NH_3 at 3300 and

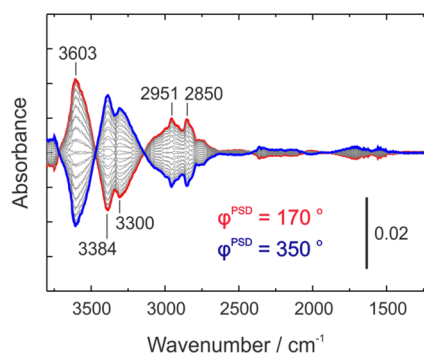


Figure 4. Phase-domain IR spectra during NH_3 modulation ($\text{NH}_3 + \text{CH}_3\text{OH} \leftrightarrow \text{CH}_3\text{OH}$) at 623 K.

3384 cm^{-1} were positive at the phase angle of 350° while the band of the methanol open dimers at 3603 cm^{-1} decreased (note that the band position shifted compared with Figure 1a because of the overlapping negative band of NH_3). Striking features were observed in the region of $1450\text{--}1650 \text{ cm}^{-1}$. Typical bands attributed to the NH deformation vibration of ammonium ions (1460 cm^{-1}), MMA (1600 cm^{-1}), and DMA (1610 cm^{-1}) adsorbed on Na^+ -MOR could not be detected;²³ only NH_3 on the Na^+ sites (1560 and 1660 cm^{-1}) was observable.²²

H^+ -MOR is reported to strongly adsorb methylamines and NH_3 as ions, which completely suppresses the adsorption of methanol under reaction conditions.²³ On the other hand, Na^+ -MOR can not only adsorb both NH_3 and methanol, but also shows rapid removal (desorption) of methylamines from the pores. Figure 5a and b shows NH_3 - and MeOH-modulated phase-domain spectra in the presence of MMA. As in Figure 5a, the addition of NH_3 (around 3450 cm^{-1}) triggered the removal of MMA highlighted by the intense negative bands at $\sim 2950 \text{ cm}^{-1}$ at a phase angle of 350° . However, MeOH removed MMA only slightly, even though MeOH dimers were formed (see Figure 5b), implying that MeOH and MMA do not share the same adsorption sites. These data clearly indicate that NH_3 is more strongly adsorbed than MMA at the reaction temperature.

Desorption of methylamines and/or scavenging of methyl groups with NH_3 (or both) have previously been suggested to be the rate-determining step of methylamine synthesis over H^+ -MOR.²³ Enhanced desorption of MMA in the presence of NH_3 leads to a strong reduction of the concentration of MMA in the pores and thereby prevents its further methylation. The relatively weak adsorption of MMA on Na^+ -MOR is therefore considered to be another crucial factor explaining the high selectivity to MMA compared with H^+ -MOR. As described above, the originally proposed shape selectivity alone is insufficient to account for the unique product distribution in methanol amination over zeolite materials. Other factors, such as the enhanced desorption of methylamines and the cleavage of the H-bond network of methanol in the micropores, have to be considered, too, for gaining deeper insight into the reaction mechanism and further fine-tuning of catalysts for the production of methylamines.

In conclusion, we have applied isotopically modulated excitation IR spectroscopy to create a chemically steady state but isotopically transient conditions at the catalytic solid–gas interface. The isotope modulation together with concentration modulation is shown to be a powerful technique to gain insight into molecular dynamics in the Na^+ -MOR pores during

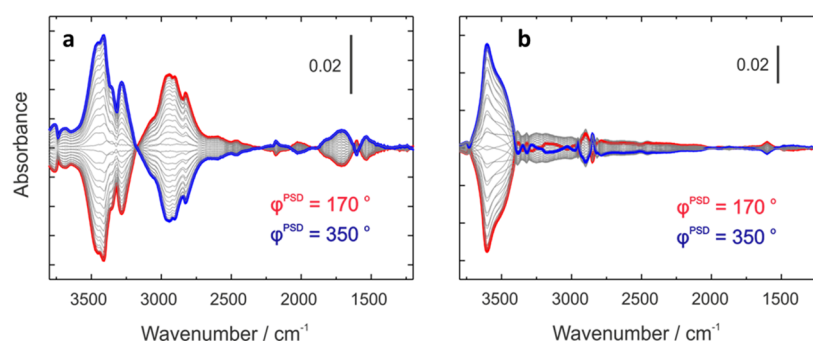


Figure 5. Phase-domain IR spectra during (a) NH_3 modulation ($\text{NH}_3 + \text{MMA} \leftrightarrow \text{MMA}$) and (b) MeOH modulation ($\text{MeOH} + \text{MMA} \leftrightarrow \text{MMA}$) at 623 K.

methanol amination for synthesis of methylamines. The studies indicate that in addition to the well-known shape-selectivity, other factors, such as the breaking of the H-bond network of methanol agglomerates and of open dimers in the Na^+ -MOR pores, may play an important role by providing NH_3 molecules access to the catalytically active sites. Furthermore, enhanced desorption of MMA by NH_3 has also been identified as a critical factor because of its role in suppressing further methylation. The weak interaction of methylamine and NH_3 with Na^+ -MOR is favorable compared with that of zeolites with strong Brønsted acid sites.

EXPERIMENTAL SECTION

Sodium cation-exchanged mordenite ($\text{SiO}_2/\text{Al}_2\text{O}_3 = 20$), JRC-Z-M20(1), was kindly supplied by the Catalysis Society of Japan. Properties of this reference material analyzed by XRD, Na^{27} and H^1 NMR, and Raman spectroscopy are given in the Supporting Information. An 80 mg portion of the mordenite powder (40–80 μm ; BET surface area, 402 m^2/g) was placed in a home-built, in situ DRIFTS cell. The design of the cell allows detecting IR signals originating from diffuse reflectance at the catalyst surface while minimizing IR absorption by gas-phase components. The inlet of the cell was connected to an air-actuated Valco valve for switching gas feeds. The concentrations in the effluent gas were monitored using an online mass spectrometer (Pfeiffer Vacuum, ThermoStar). DRIFT spectra were measured on a Bruker Equinox 55 FT-IR spectrometer equipped with a liquid-nitrogen-cooled MCT detector at 4 cm^{-1} resolution. MES experiments were carried out by periodically switching between two different gas atmospheres. For each MES measurement, the cycles were repeated nine times, and the last six cycles were averaged to enhance the S/N ratio. The acquired time-domain spectra were mathematically treated by PSD according to

$$A_k(\tilde{\nu}) \cos(\varphi_k + \varphi_k^{\text{delay}}(\tilde{\nu})) = \frac{2}{T} \int_0^T A(t, \tilde{\nu}) \sin(k\omega t + \varphi_k) dt \quad (1)$$

where T is the length of a cycle, ω is the demodulation frequency, φ_k is the demodulation phase angle, k is the demodulation index ($k = 1$ in this study), and $A(t, \tilde{\nu})$ and $A_k(\tilde{\nu})$ are the active species responses in time and phase domain, respectively.

Prior to catalytic reaction, the mordenite powders were pretreated in situ with 5 vol % O_2 in He at 723 K for 3 h (until the MS signals of CO_2 and H_2O disappeared completely). The isotope-modulation experiments were carried out at 523–623

K by switching between two different effluent gases: 16.7 vol % CH_3OH in a He balance and 16.7 vol % CD_3OD in a He balance in the absence or presence, respectively, of 16.7 vol % NH_3 (nitrogen to carbon ratio = 1).

ASSOCIATED CONTENT

Supporting Information

Catalyst composition, XRD pattern, NMR data, and Raman spectrum of catalyst. IR spectrum of MMA. This information is available free of charge via the Internet at <http://pubs.acs.org>.

AUTHOR INFORMATION

Corresponding Author

*E-mail: nobutaka.maeda@chem.ethz.ch, baiker@chem.ethz.ch.

Notes

The authors declare no competing financial interest.

ACKNOWLEDGMENTS

We thank Dr. René Verel for the NMR characterization of the Na^+ -MOR and H^+ -MOR samples. Thanks is also due to Dr. Robert Büchel for providing data on the BET surface area, XRD pattern, and a Raman spectrum.

REFERENCES

- Bizzari, S. N. *Chemical Economics Handbook*; SRI Consulting: Menlo Park, CA, 2008.
- Hayes, K. S. *Appl. Catal., A* **2001**, 221, 187.
- Corbin, D. R.; Schwarz, S.; Sonnichsen, G. C. *Catal. Today* **1997**, 37, 71. Hayes, K. S. *Appl. Catal., A* **2001**, 221, 187–195.
- Tijsebaert, B.; Yilmaz, B.; Muller, U.; Gies, H.; Zhang, W. P.; Bao, X. H.; Xiao, F. S.; Tatsumi, T.; Vos, D. D. *J. Catal.* **2011**, 278, 246.
- Veeffkind, V. A.; Grundling, C.; Lercher, J. A. *J. Mol. Catal. A: Chem.* **1998**, 134, 111.
- Carja, G.; Nakamura, R.; Niiyama, H. *Appl. Catal., A* **2002**, 236, 91.
- Abrams, L.; Corbin, D. R. *J. Incl. Phenom. Mol. Recognit. Chem.* **1995**, 21, 1.
- Weigert, F. J. *J. Catal.* **1987**, 103, 20.
- Keane, M.; Sonnichsen, G. C.; Abrams, L.; Corbin, D. R.; Gier, T. E.; Shannon, R. D. *Appl. Catal.* **1987**, 32, 361.
- Meunier, F. C. *Chem. Soc. Rev.* **2010**, 39, 4602.
- Meunier, F. C. *Catal. Today* **2010**, 155, 164.
- Jacobs, G.; Davis, B. H. *Appl. Catal., A* **2007**, 333, 192.
- Olympiou, G. G.; Kalamaras, C. M.; Zeinalipour-Yazdi, C. D.; Efstathiou, A. M. *Catal. Today* **2007**, 127, 304.
- Schweicher, J.; Bundhoo, A.; Frennet, A.; Kruse, N.; Daly, H.; Meunier, F. C. *J. Phys. Chem. C* **2010**, 114, 2248.
- Baurecht, D.; Fringeli, U. P. *Rev. Sci. Instrum.* **2001**, 72, 3782.

- (16) Urakawa, A.; Bürgi, T.; Baiker, A. *Chem. Eng. Sci.* **2008**, *63*, 4902.
- (17) Bertie, J. E.; Zhang, S. L. L. *J. Mol. Struct.* **1997**, *413*, 333.
- (18) Michalak, D. J.; Rivillon, S.; Chabal, Y. J.; Esteve, A.; Lewis, N. S. *J. Phys. Chem. B* **2006**, *110*, 20426.
- (19) Wu, X.; Chen, Y.; Yamaguchi, T. *J. Mol. Spectrosc.* **2007**, *246*, 187.
- (20) Provencal, R. A.; Paul, J. B.; Roth, K.; Chapo, C.; Casaes, R. N.; Saykally, R. J.; Tschumper, G. S.; Schaefer, H. F. *J. Chem. Phys.* **1999**, *110*, 4258.
- (21) Huisken, F.; Kaloudis, M.; Koch, M.; Werhahn, O. *J. Chem. Phys.* **1996**, *105*, 8965.
- (22) Schenkel, R.; Olindo, R.; Kornatowski, J.; Lercher, J. A. *Appl. Catal., A* **2006**, *307*, 108.
- (23) Grundling, C.; EderMirth, G.; Lercher, J. A. *J. Catal.* **1996**, *160* (299), 49.